Fabrication of High Aspect Ratio and Open-Ended TiO_2 Nanotube Photocatalytic Arrays Through Electrochemical Anodization

Roong Jien Wong, Sanly Liu, Yun Hau Ng, and Rose Amal
Particle and Catalysis Research Group, School of Chemical Engineering, The University of New South Wales, Sydney, NSW 2052, Australia

DOI 10.1002/aic.15117
Published online December 31, 2015 in Wiley Online Library (wileyonlinelibrary.com)

Well-aligned, high aspect-ratio and open-ended TiO_2 nanotube arrays secured within a Ti foil (TiO_2 nanotubes cartridge) were successfully prepared through the double-sided anodization method. With ~210 μm of nanotube length, the anodic growth of TiO_2 was accelerated and stabilized by the lactic acid-containing ethylene glycol electrolyte. In the absence of lactic acid, the anodization led to detachment of nanotubes from the Ti foil after 5–6 h of high voltage (80 V) anodization. Transmission electron microscope image and Raman spectrum revealed that the as-anodized TiO_2 nanotube arrays without annealing treatment were partially crystalline anatase and demonstrated photocatalytic activity in the mineralization of formic acid. © 2015 American Institute of Chemical Engineers *AIChE J*, 62: 415–420, 2016
Keywords: TiO2 nanotube, anodization, photocatalyst, electrochemical, flow through

Introduction

TiO_2 has demonstrated potentials for photocatalysis, water splitting, dye-sensitized solar cells, electrochromic materials, and biomedical applications. After the breakthrough discovery in anodic growth of highly ordered porous alumina (Al_2O_3) membrane by Masuda and Fukuda[1] in 1995, research in fabricating well-aligned TiO_2 nanotubes (TiNT) using anodization have attracted considerable attention in TiO_2-field community. This is mainly attributed to the expectation of significantly improved charge transport properties in nanomaterials with one-dimensional (1-D) structure.[2] Many groups including Schmuki and Grimes have done comprehensive and groundbreaking works in the area of anodization of Ti including the investigation of the growth mechanism,[3–5] control of the morphological features,[5–9] tuning of the composition (e.g., Ti-Fe-O nanotubes or Cu-Ti-O),[10,11] and the applications of these tubular TiO_2.[12,13] Based on the direct anodization method, the obtained TiO_2 nanotubes are well-aligned on the Ti substrate where the bottom of the nanotubes is attached on and closed by the Ti substrate. Depending on the targeted applications, opening of the bottom-end of the TiO_2 nanotubes can offer several desired properties such as the flow-through type biofilter,[14,15] double-side illumination system for photoelectrocatalytic hydrogen generation through water splitting using solar energy[16] and flow-through photocatalytic membrane.[17–19]

Various methods involving anodization have been reported for the fabrication of flow-through TiNT membrane mainly by chemically opening the closed bottom end of the TiNT array. Prior to the chemical dissolution of the closed bottom end, free-standing TiNT arrays were first obtained either by selective metal dissolution,[18] by chemical assisted separation,[20] by applying reverse bias,[21] or by ultrasonic agitation[22–24] to detach the NT arrays from the metal substrate. The detached TiNT arrays were then exposed to hazardous chemicals such as HF acid solution and vapour,[18,22] oxalic acid solution,[25] and NH_4F – H_2SO_4 solution[23] for suitable time length to obtain flow-through TiNT membranes. However, it was observed that the bottom morphology of the nanotube was not homogeneous after pore-opening.[18] Inductively coupled plasma etching was also used to open the nanotube pores.[26] Kant and Losic have reported successful fabrication of free-standing flow-through TiNT membrane by gradually reducing the anodization potential at the end of anodization process to reduce the formation of the oxide layer resulted in the nanotubes opened at the bottom after detachment from the Ti surface.[27] A few reports have shown reproducible and reliable results with an abrupt increase in the potential at the end of anodization, which allowed the pores to homogeneously open in the barrier layer.[28–30] The aforementioned methods of preparing flow-through TiNT membrane produce freestanding membranes. Further steps are required to transfer the free-standing membrane onto a solid support before the membrane can be used due to the brittle nature of the material. This further step taken to reattach the TiNT membrane on other solid substrate defeats the purpose of creating an open-ended membrane. Other than that, freestanding nanotube membranes face the challenges of material handling. Without a solid support, the as-prepared freestanding flow-through TiNT membranes

Additional Supporting Information may be found in the online version of this article.

Correspondence concerning this article should be addressed to Y. H. Ng at yh.ng@unsw.edu.au or R. Amal at r.amal@unsw.edu.au.

may be easily broken during sample preparation and transfer. Fabrication of freestanding flow-through TiNT membrane also raises safety concerns when hazardous chemicals such as HF acid is used, while the option of using inductively coupled plasma etching is only practical for laboratory scale experiments.

Alternatively, the notion of applying a sacrificial conductive layer at the bottom of the Ti metal substrate to remove the barrier layer directly during anodization was demonstrated in the works of Albu et al.[31] and Zhang et al.[32] In Albu et al.'s work, aluminium was deposited on the Ti foil by electron beam evaporation, a technique that requires low operating pressure. The aluminium/alumina layer was removed with acid solution afterward to obtain the flow-through TiNT membrane framed within the metal substrate, hence allowing it to be used immediately without the need of transferring the membrane onto another solid support. Nevertheless, several disadvantages of the reported methods in literature have been identified. The anodization step alone may take up to several days to fabricate TiNT membranes with tube length >100 μm. Thick TiNT membranes will have high surface roughness, which is desirable in catalysis and photocatalysis as it provides more reaction sites as well as longer retention time within the tubular structure. Although the reported use of a sacrificial conductive layer may have solved most of the issues, depositing aluminium by electron beam evaporation is not feasible for larger scale production.

In this work, a flow-through TiNT membrane is prepared via an accelerated direct anodization method coupled with electrodeposition and acid dissolution. Lactic acid is used to allow the fabrication of TiNT membrane at high applied potential by preventing dielectric breakdown.[33] A metallic zinc sacrificial layer, which can be easily removed with dilute H_2SO_4, is deposited onto the Ti metal substrate via electrodeposition to achieve flow-through morphology. On top of that, the flow-through TiNT membrane presented in this work is buried within the Ti metal support, hence ensuring 1-D growth of nanotube structure as well as protecting the TiNT from external shear forces. This method of fabrication will eliminate the need of transferring the freestanding membrane onto a solid support to facilitate easier handling.

Experimental

Materials and reagents

Aldrich titanium foil (0.127 mm thick, 99.7% metal basis) was used for the synthesis of TiNT arrays. Titanium foil was cut into 3 cm $\times$ 3 cm square foils, and was cleaned using acetone (Ajax, >99.5%) and Milli-Q water. The Ti foils were immersed in acetone and cleaned under water bath ultrasonication for 5 min. The Ti foils were then further cleaned by ultrasonication in Milli-Q water for another 5 min under ultrasonication before being rinsed with Milli-Q water. The cleaned Ti foils were dried at 110°C overnight and were wrapped in aluminium foils for storage in vacuum desiccator.

TiNT arrays were prepared using ethylene glycol based fluoride electrolyte. 100 g of electrolyte was prepared for each anodization, comprising 94.5 wt % ethylene glycol (Aldrich, *ReagentPlus®*, >99%), 5 wt % Milli-Q water, and 0.5 wt % sodium fluoride (Ajax, >99%). The electrolyte mixture was evenly dispersed using an ultrasonic water bath for 1 min and was stirred at 500 rpm for 5 min.

Preparation of flow through TiO_2 nanotube membrane

A piece of Ti foil was placed at the bottom of a cylindrical Teflon cell as the working electrode (anode) with total exposed area of 3.80 cm^2, and a platinum foil was used as the counter electrode (cathode). A schematic illustration of the anodization reactor can be seen in Supporting Information Figure S1 in the supporting information. Anodization of Ti foil in preparation of TiNT arrays was performed under constant applied potential of 60 V between the electrodes (Ti and Pt) for 20 h using a programmable DC power supply (PST-3201 GW Instek) interfaced with a computer. A mechanical glass stirrer was used to ensure homogeneity of the electrolyte. The as-prepared TiNT array was removed after 20 h of anodization and was rinsed with Milli-Q water to remove all electrolyte residues. After the first anodization step, another anodization of the Ti foil was performed to the opposite side at 60 V for 20 h. The TiNT arrays were subsequently removed, to produce a clean Ti foil template with cavities. The purpose of producing the cavities on the Ti foil was to contain the nanotube array within the Ti foil, and hence using the Ti foil as a support to improve handling and mechanical strength of the TiNT membrane. Prior to the third anodization, a layer of Zn was coated on the bottom surface of the Ti foil to serve as a conducting substrate during the final stage of the third anodization. 100 mL of 50 mM $ZnSO_4.7H_2O$ was used as the electrolyte. Pt foil was used as the counter electrode and Ti foil was used as the working electrode. Electrodeposition of Zn was carried out for 1 h with an applied bias of -1 V and was monitored with an Autolab PGSTAT302N potentiostat. The Zn deposited Ti foil was then rinsed with Milli-Q water to remove any $ZnSO_4$ residue, and was dried under ambient condition.

During the third anodization step, 1 g of lactic acid was added into the electrolyte, which has been pre-aged for 40 h. The Zn deposited Ti foil was placed at the bottom of the Teflon anodization cell, with the Zn deposited surface facing down. The electrolyte was preheated to 60°C before being transferred into the anodization cell. The anodization was performed at 80 V applied potential for 45 h to achieve complete consumption of Ti foil for TiNT growth. A wool insulation jacket was used to help maintain the temperature of the electrolyte during anodization. 0.1 M H_2SO_4 was used to dissolve the remaining Zn after the third anodization to achieve flow-through TiNT membrane structure.

Characterization method

XRD analysis of as-anodized TiO_2 nanotubes array in thin film mode was performed using PANalytical X'Pert MPD with a slight modification of the sample holder. The X-ray operating conditions were 45 kV and 40 mA. Morphology and thickness of the TiNT array were studied using Scanning Electron Microscopy (SEM, FEI Nova NanoSEM 230) and Transmission Electron Microscopy (TEM, FEI Tecnai G2 20 TEM). TiNT samples were cut and attached to a copper grid using conductive carbon tapes. The samples were sputter-coated with chromium using the Emitech K550x Chromium Sputter Coater prior to SEM imaging. Elemental composition of the samples was analyzed using energy-dispersive spectroscopy (EDS) and the data was analysed using Esprit EDS software. Before EDS analysis, the samples were coated with carbon.

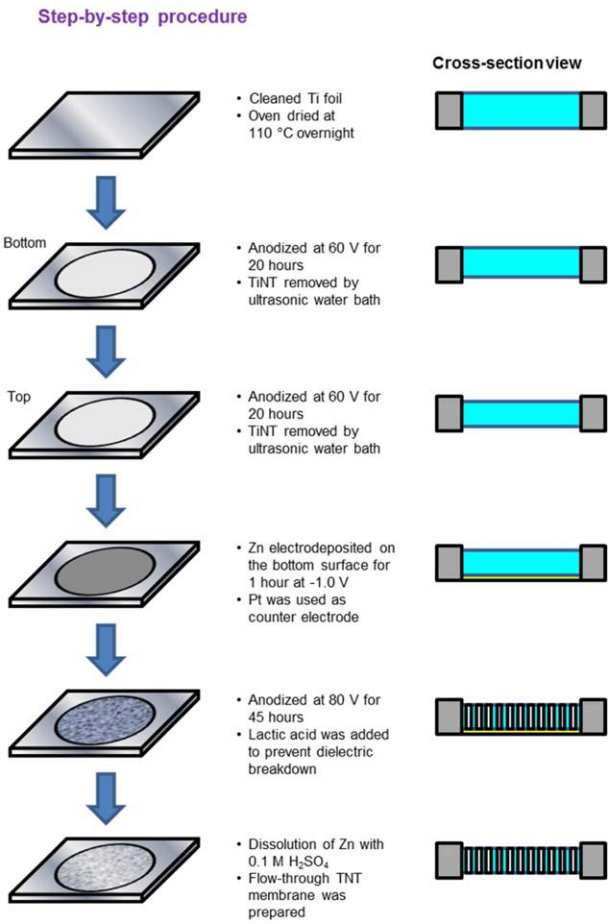

Figure 1. Step by step procedure for the fabrication of TiO_2 nanotubes "cartridge."

[Color figure can be viewed in the online issue, which is available at wileyonlinelibrary.com.]

Results and Discussion

As illustrated in Figure 1, flow through TiO_2 nanotube arrays were prepared in a three step electrochemical anodization process, in which titanium foils act as anode and metal Pt as a counter electrode. Sodium fluoride was used as the complexation etching source to induce mild chemical dissolution of the oxide formed, instead of the more toxic hydrofluoric acid and ammonium fluoride. In the beginning of the anodization process, the metallic surface of the anodized area was oxidized, releasing Ti^{4+} ions, and electrons. The chemical interaction of the released Ti^{4+} ions and O^{2-} ions forms TiO_2, while reactions with OH^- ions of water molecules forms hydrated anodic layer ($Ti(OH)_4$), which then produces TiO_2 via a condensation reaction. The fluoride ions in the electrolyte attack the hydrated and the oxide layers, resulting in the creation of small pits, which converts into pores uniformly distributed over the whole surface. The as-formed TiO_2 layer in the first step was peeled off by ultrasonication to expose the substrate, and then the opposite side of the patterned substrate was subjected to another anodization and TiO_2 removal cycle. Prior to the third anodization step, a layer of Zn was coated on one side of the patterned Ti foil to serve as a conducting substrate during the final stage of the third anodization. During the third anodization step, lactic acid was added to the electrolyte to prevent dielectric breakdown, which then allowed the anodization procedure to be performed at higher applied bias (80 V).[33] As mentioned, the patterned pits induced by the mild chemical dissolution worked as pore nucleation centers for the successive growth of homogeneous pores of nanotubes. Eventually, growth of the pores occurred inward toward the underneath Zn metal-oxide interface until a nanotubular structure was developed and full consumption of the Ti foil occurred, leading to the formation of flow through TiNT membrane. Acid dissolution was performed to remove residual Zn.

The growth of TiNT can be monitored from the current-time profile during anodization process (Figure 2a). Before the anodization started, a high current of 68 mA was observed because of the high conductivity between the interface of the electrolyte and the titanium foil. At the initial stage of the anodization process, a current rapidly drop to below 40 mA within the first minute of anodization due to the oxidation of Ti foil to form a thin compact titanium dioxide layer.[34] The compact oxide layer reduced the exposed surface area of titanium metal and limited the ionic current as the Ti^{4+} ions and O^{2-} ions have to migrate through the barrier layer to react. Subsequently, a bounce back in current was observed when chemical dissolution of the metal oxide layer by fluoride ions in the electrolyte started to take place, which exposed more titanium metal available for oxidation. As the oxide formation and chemical dissolution reactions occurred concurrently and approached equilibrium, the anodization current reached a steady state between 8000 s and 18,500 s. As previously observed, penetration to the underlayer metal will result in a current drop in the anodization profile.[32] Therefore, after 18,500 s (the point where the current started to decrease), opening of the bottom nanotube was believed to occur,

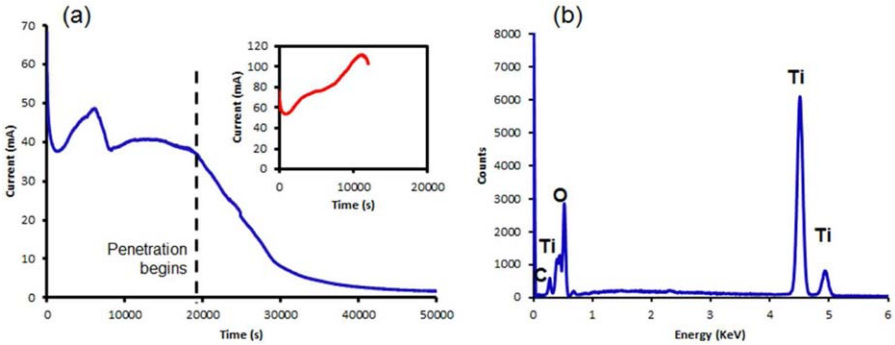

Figure 2. (a) Current-time profile during the preparation of flow-through TiNT membrane. Inset shows the anodization in the absence of lactic acid; (b) EDS spectrum of the resultant TiNT membrane on Zn removal.

[Color figure can be viewed in the online issue, which is available at wileyonlinelibrary.com.]

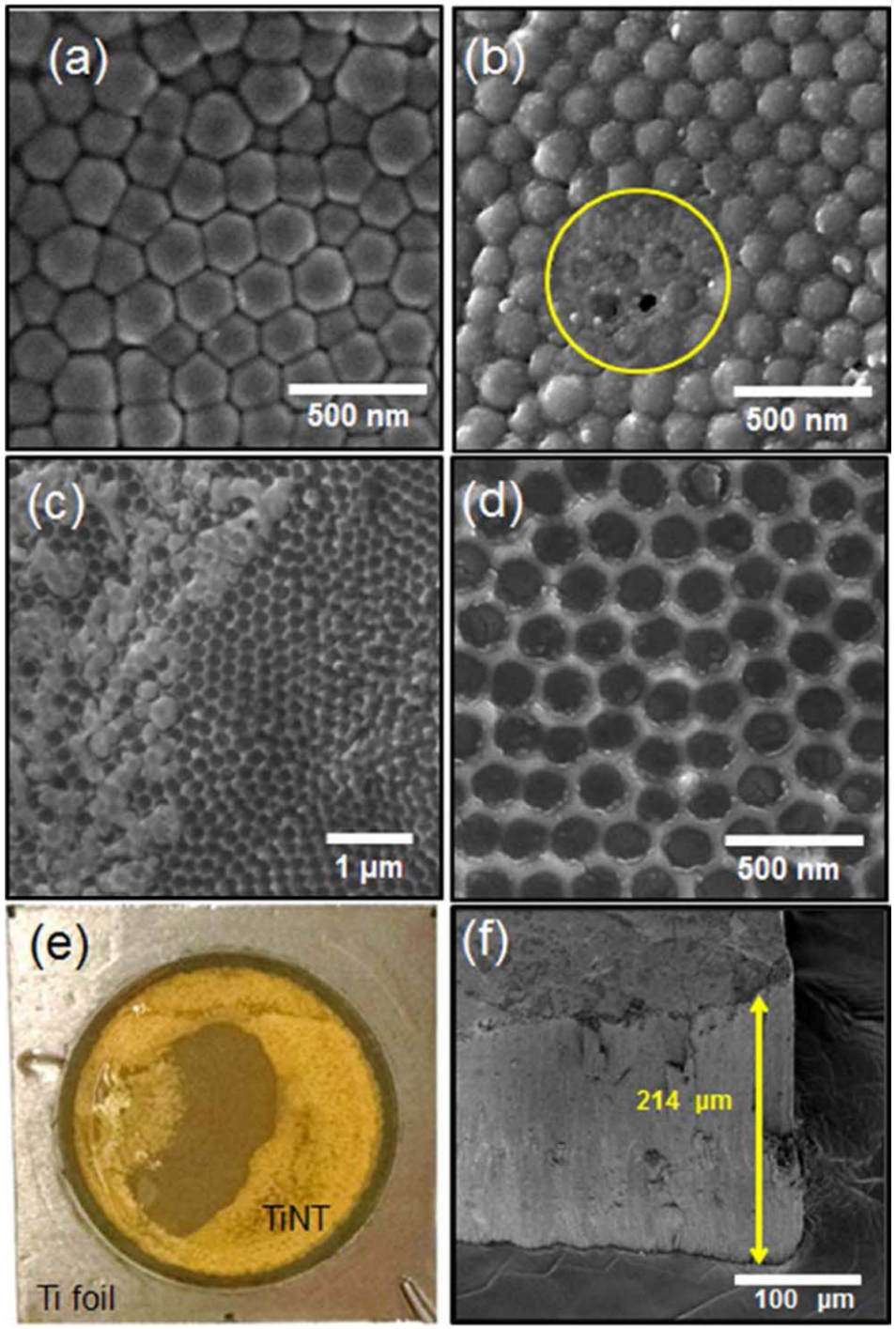

Figure 3. SEM images of the bottom surface of TiO_2 nanotube structures before (a) and after the third anodization step showing (b) the initial stage of opening of the TiO_2 nanotube, (c) partially opened TiNT membrane, and (d) fully-opened flow through TiNT membrane, (e) photograph of the TiNT encapsulated within Ti foil, and (f) length of the anodized TiNT array.

[Color figure can be viewed in the online issue, which is available at wileyonlinelibrary.com.]

resulting in a gradually but fully opened flow-through TiNT membrane after 45,000 s (when the current reached another stable reading). Noticeably, lactic acid is a critical additive in electrolyte in ensuring the formation of thick and stable TiNT arrays formed at the high voltage of 80 V. In the absence of lactic acid at this voltage, the anodization process proceeded in an uncontrolled manner in which significant chemical dissolution of oxide took place and resulted in the detachment of nanotube arrays after around 8 h of anodization. Along with the peeling off observation, this uncontrolled anodization was also evident with the ever increasing anodic current during the anodization (inset of Figure 2a), which is an indication of severe chemical dissolution of TiO_2. Therefore, the use of lactic acid allows a thicker film to be formed and stabilized. On completion of the anodization process, the underlayer Zn component was conveniently removed using dilute H_2SO_4. EDS

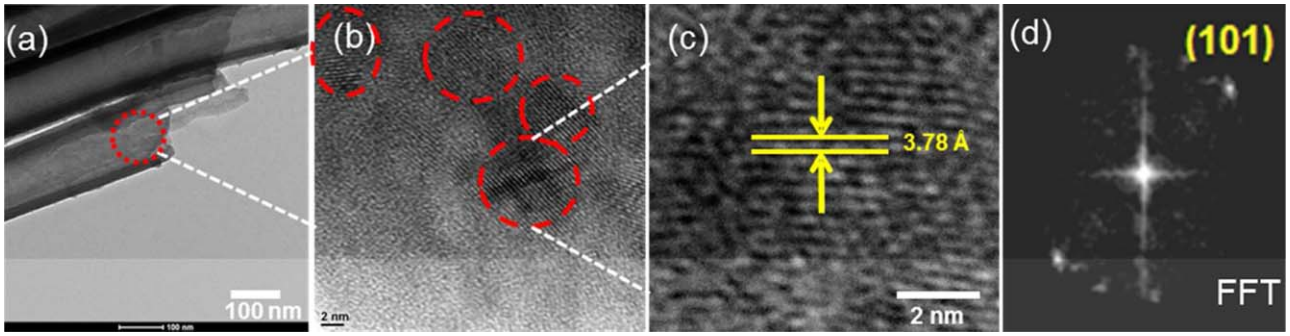

Figure 4. TEM images (a–c) of as-anodised TiNT membrane and its corresponding FFT analysis (d).

[Color figure can be viewed in the online issue, which is available at wileyonlinelibrary.com.]

analysis spectrum of the resultant TiNT is showed in Figure 2b. Elemental Ti, O, and trace C were the only elements present without the detection of Zn.

Figure 3a shows the bottom surface of densely packed TiNT array after the Zn electrodeposition step with the end of the nanotubes still closed. With the third anodization step, a surface morphology consisting of ring-like structure was observed, indicating the initial stage of opening of the nanotubes (Figure 3b). Figures 3c, d show the bottom surface of the TiNT array membranes with partially and fully opened through-hole morphology, respectively. Top view of the TiNT array can be seen in Supporting Information Figure S2 which represents the typical well-aligned tubular structure of anodized TiO_2. Combining the top and bottom view SEM images confirm the formation of open-ended flow-through TiNT array. The configuration of this array of tubular TiO_2 being fastened by the surrounding Ti foil is principally functioned as a TiO_2 nanotubes "cartridge" which could be conveniently inserted and withdrawn from tailor-made reactors. Figure 3e shows the photograph of this TiNT cartridge. The yellow component framed within the metallic Ti foil is the flow-through TiO_2 nanotube arrays. Water can be evidently diffused through the nanotubes in separate experiments (Supporting Information Figure S3). For typical anodization of Ti foil, the non-opened (one-side anodized) TiO_2 nanotube usually present greyish colour as the underlayer of Ti foil is opaque. While the length of TiNT array can be controlled by selecting the thickness of Ti foil as well as the duration of the first and second step anodization, the overall length of the TiNT array prepared under this experimental condition is ca. 214 μm as shown in Figure 3f.

It is worth to note that the open-ended flow-through TiNT array obtained from this procedure was not subject to calcination for crystallization. It is therefore expected that the TiNT membrane will not demonstrate long range order of crystal structure (Please refer to Supporting Information Figure S4 in the supporting information for the XRD patterns of the TiNT membrane). Although some applications such as filtration based on sieving principles do not require crystalline membranes, a certain degree of crystallinity is needed for other applications involving electrical charge carrier generation and transport/transfer, including photocatalytic cleaning. TEM image in Figure 4a shows that the TiNT has 1-D assembly with hollow tubular structure. Multiple regions with short-range order in Figure 4b clearly indicate the existence of certain degree of crystallinity within this as-anodised TiNT membrane. Examination of the wall of the TiNT under high magnification (Figure 4c) reveals the presence of lattice fringe of 0.37 nm along the (101) plane of anatase TiO_2. Its corresponding FFT image also confirms the formation of anatase. The presence of crystals may be related to local dielectric breakdown occurring within a small section of the film during the growth. The observation of fractionally crystalline anatase phase on uncalcined TiNT was also previously reported by Grimes[35] and Schmuki.[3] Grimes and coworkers reported that the control of anodization process may enable the direct formation of crystalline nanotube arrays without annealing. Schmuki et al. reported that the anodization at 40 V afforded poorly crystalline anatase (while 20 V yielded a total amorphous phase). It is therefore reasonable that the higher anodization voltage (80 V) employed in this work to contribute to the formation of anatase. In addition to HRTEM analysis, result from Raman analysis is also in good agreement (Supporting Information Figure S5). Although the peaks are not well-defined, the Raman spectrum indicates the presence of typical vibration modes for anatase at the relevant Raman shift. This feature is interesting, as to the best of our knowledge, this is for the first time an open-ended flow-through TiNT membrane prepared without thermal treatment might demonstrate photoactivity owing to the crystallinity. To probe it, preliminary testing of photocatalytic activity of the TiO_2 nanotube was carried out using formic acid as the model organic compound (Please refer to Figure S6 in Supporting Information). The result showed that the as-prepared TiNT is photocatalytically active to mineralize formic acid into CO_2 under UV illumination even without a calcination treatment (Supporting Information Figure S6). This result verifies the potential use of TiNT membrane in photocatalytic applications. More work is currently underway to design a novel reactor system that can fully claim the advantage of flow-through TiNT as a "cartridge."

Conclusion

In summary, we have developed a facile fabrication method of large area TiO_2 NT array secured within a Ti foil (TiO_2 nanotubes cartridge) with through-hole morphology. The process reported here is very simple and environmentally friendly. The configuration of TiO_2 NT array membranes being fastened by the surrounding Ti foil could be conveniently inserted and withdrawn from tailor-made reactors. With proper reactor engineering, TiO_2 nanotubes cartridge configuration can find potential applications in flow-through biofilter and photocatalytic membranes, various photoelectric devices and nanoreactors.

Acknowledgments

This work was financially supported by the Australian Research Council (DP110101638). The authors would like to

acknowledge the UNSW Mark Wainwright Analytical Centre for providing facility and technical supports.

Literature Cited

1. Masuda H, Fukuda K. Ordered metal nanohole arrays made by a two-step replication of honeycomb structures of anodic alumina. *Science*. 1995;268(5216):1466–1468.
2. Zhu K, Neale RN, Miedaner A, Frank AJ. Enhanced charge-collection efficiencies and light scattering in dye-sensitized solar cells using oriented TiO2 nanotubes arrays. *Nano Lett*. 2007;7(1): 69–74.
3. Jaroenworaluck A, Regonini D, Bowen CR, Stevens R, Allsopp D. Macro, micro and nanostructure of TiO2 anodised films prepared in a fluorine-containing electrolyte. *J Mater Sci*. 2007;42(16):6729–6734.
4. Macak J, Hildebrand H, Marten-Jahns U, Schmuki P. Mechanistic aspects and growth of large diameter self-organized TiO 2 nanotubes. *J Electroanal Chem*. 2008;621(2):254–266.
5. Berger S, Hahn R, Roy P, Schmuki P. Self-organized TiO2 nanotubes: factors affecting their morphology and properties. *Phys Status Solidi (b)*. 2010;247(10):2424–2435.
6. Seyeux A, Berger S, LeClere D, Valota Anna, Skeldon P, Thompson GE, Kunze J, Schmuki P. Influence of surface condition on nanoporous and nanotubular film formation on Titanium. *J Electrochem Soc*. 2009;156(2):K17–K22.
7. Berger S, Tsuchiya H, Schmuki P. Transition from nanopores to nanotubes: self-ordered anodic oxide structures on titanium−aluminides. *Chem Mater*. 2008;20(10):3245–3247.
8. Wei W, Berger S, Hauser C, Meyer K, Yang M, Schmuki P. Transition of TiO 2 nanotubes to nanopores for electrolytes with very low water contents. *Electrochem Commun*. 2010;12(9):1184–1186.
9. Albu SP, Roy P, Virtanen S, Schmuki P. Self-organized TiO2 nanotube arrays: critical effects on morphology and growth. *Isr J Chem*. 2010;50(4):453–467.
10. Mor GK, Prakasam HE, Varghese OK, Shankar K, Grimes CA. Vertically oriented Ti-Fe-O nanotube array films: toward a useful material architecture for solar spectrum water photoelectrolysis. *Nano Lett*. 2007;7(8):2356–2364.
11. Mor GK, Varghese OK, Wilke RH, Sharma S, Shankar K, Latempa TJ, Choi KS, Grimes CA. p-Type Cu−Ti−O nanotube arrays and their use in self-biased heterojunction photoelectrochemical diodes for hydrogen generation. *Nano Lett*. 2008;8(7):1906–1911.
12. Mor GK, Shankar K, Paulose M, Varghese OK, Grimes CA. Use of highly-ordered TiO2 nanotube arrays in dye-sensitized solar cells. *Nano Lett*. 2006;6(2):215–218.
13. Grimes CA. Synthesis and application of highly ordered arrays of TiO2 nanotubes. *J Mater Chem*. 2007;17(15):1451–1457.
14. Liu G, Wang K, Hoivik N, Jakobsen H. Progress on free-standing and flow-through TiO_2 nanotube membranes. *Sol Energy Mater Sol Cells*. 2012;98:24–38.
15. Schweicher J, Desai TA. Facile synthesis of robust free-standing TiO2 nanotubular membranes for biofiltration applications. *J Appl Electrochem*. 2014;44(3):411–418.
16. Mohapatra SK, Mahajan VK, Misra M. Double-side illuminated titania nanotubes for high volume hydrogen generation by water splitting. *Nanotechnology*. 2007;18(44):445705.
17. Lin C-J, Yu W-Y, Lu Y-T, Chien S-H. Fabrication of open-ended high aspect-ratio anodic TiO2 nanotube films for photocatalytic and photoelectrocatalytic applications. *Chem Commun*. 2008;(45):6031–6033.
18. Albu SP, Ghicov A, Macak JM, Hahn R, Schmuki P. Self-organized, free-standing TiO2 nanotube membrane for flow-through photocatalytic applications. *Nano Lett*. 2007;7(5):1286–1289.
19. Liao J, Lin S, Pan N, Li D, Li S, Li J. Free-standing open-ended TiO_2 nanotube membranes and their promising through-hole applications. *Chem Eng J*. 2012;211:343–352.
20. Chen X, Mao SS. Titanium dioxide nanomaterials: synthesis, properties, modifications, and applications. *Chem Rev*. 2007;107(7):2891–2959.
21. Liao JJ, Lin SW, Pan NQ, Cao XK, Li JB. Facile fabrication of open-ended high aspect-ratio anodic TiO2 nanotube films and their applications. In: Pan W, Gong JH, editors. *High-Performance Ceramics VII, Pts 1 and 2,* Vol. 512–515, Switzerland: Trans Tech Publications, 2012:1659–1662.
22. Paulose M, Prakasam HE, Varghese OK, Peng L, Popat KC, Mor GK, Desai TA, Grimes CA. TiO2 nanotube arrays of 1000 μm length by anodization of titanium foil: phenol red diffusion. *J Phys Chem C*. 2007;111(41):14992–14997.
23. Fang D, Huang K, Liu S, Qin D. High density copper nanowire arrays deposition inside ordered titania pores by electrodeposition. *Electrochem. Commun*. 2009;11(4):901–904.
24. Lei B-X, Liao J-Y, Zhang R, Wang J, Su C-Y, Kuang D-B. Ordered crystalline TiO2 nanotube arrays on transparent FTO glass for efficient dye-sensitized solar cells. *J Phys Chem C*. 2010;114(35): 15228–15233.
25. Lin C-J, Yu W-Y, Lu Y-T, Chien S-H. Fabrication of open-ended high aspect-ratio anodic TiO2 nanotube films for photocatalytic and photoelectrocatalytic applications. *Chem Commun*. 2008;0(45):6031–6033.
26. Zhu B, Li JJ, Chen QW, Cao RG, Li JM, Xu DS. Artificial, switchable K+-gated ion channels based on flow-through titania-nanotube arrays. *Phys Chem Chem Phys*. 2010;12(34):9989–9992.
27. Kant K, Losic D. A simple approach for synthesis of TiO2 nanotubes with through-hole morphology. *Phys Status Solidi Rapid Res Lett*. 2009;3(5):139–141.
28. Jo Y, Jung I, Lee I, Choi J, Tak Y. Fabrication of through-hole TiO2 nanotubes by potential shock. *Electrochem Commun*. 2010; 12(5):616–619.
29. Liao JJ, Lin SW, Pan NQ, Li SP, Cao XK, Cao Y. Fabrication and photocatalytic properties of free-standing TiO2 nanotube membranes with through-hole morphology. *Mater Charact*. 2012;66:24–29.
30. Wang D, Liu L. Continuous fabrication of free-standing TiO2 nanotube array membranes with controllable morphology for depositing interdigitated heterojunctions. *Chem Mater*. 2010;22(24):6656–6664.
31. Albu SP, Ghicov A, Berger S, Jha H, Schmuki P. TiO2 nanotube layers: flexible and electrically active flow-through membranes. *Electrochem Commun*. 2010;12(10):1352–1355.
32. Zhang ZK, Guo DZ, Xing YJ, Zhang GM. Fabrication of open-ended TiO2 nanotube arrays by a simple two-step anodization. *Phys Status Solidi Rapid Res Lett*. 2010;4(11):299–301.
33. So S, Lee K, Schmuki P. Ultrafast growth of highly ordered anodic TiO2 nanotubes in lactic acid electrolytes. *J Am Chem Soc*. 2012; 134(28):11316–11318.
34. Yun J-H, Ng YH, Ye C, Mozer AJ, Wallace GG, Amal R. Sodium fluoride-assisted modulation of anodized TiO2 nanotube for dye-sensitized solar cells application. *ACS Appl Mater Interfaces*. 2011; 3(5):1585–1593.
35. Yoriya S, Mor GK, Sharma S, Grimes CA. Synthesis of ordered arrays of discrete, partially crystalline titania nanotubes by Ti anodization using diethylene glycol electrolytes. *J Mater Chem*. 2008; 18(28):3332–3336.

Manuscript received Aug. 20, 2015, and revision received Nov. 6, 2015.